SUPPLEMENTARY MATERIAL

Fig. S1

1. TALEEEIK
2. ANTLSQLSK
3. KLIIDVIR
4. LREEVVTK
5. IYDVEQTR
6. YGSIVDDER
7. TEISLVLTSK
8. IVGNLLYYR
9. SPAIGLNNLDK
10. FQATSSGPILR
11. GIAEQTVVTLR
12. FPDATEDELLK
13. LGIAPQIQDLLGK
14. YDIEDGEAIDSR
15. NKLEASIENLRR
16. SFLHEQEENVVK
17. SLIINTNPVEVYK
18. TLVGSENPPLTVIR
19. ENIWSASEELLLR
20. KSFLHEQEENVVK
21. AWVNQLETQTGEASK
22. GVLLDIDDLQTNQFK
23. VDQVQDIVTGNPTVIK
24. EIEDIIEEVTVGYIR
25. VLNSIISSLDLLPYGLR
26. VVAVGYINEAIDEGNPLR
27. SKVDQVQDIVTGNPTVIK
28. LPYDVTTEQALTYPEVK
29. NPNAVLTLVDDNLAPEYQK
30. ARDDYKTLVGSENPPLTVIR
31. VLWLDEIQQAVDEANVDEDR
32. QAAVDHINAVIPEGDPENTLLALK
33. TALQEEIK
34. TLSALLLPAAGLDDVSLPVAPR
35. FAHLLNQSQQDFLAEAELLK
36. AQELGLVELLEKEEVQAGVAAANTK

Fig. S1. Peptides identified by mass spectrometry. A total of 36 peptides were identified by tandem MS/MS corresponding to IQ-domain GTPase Activating Proteins (IQGAPs).

Fig. S2

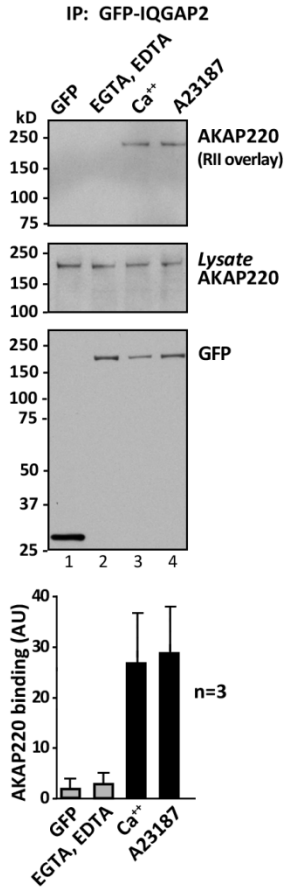

Fig. S2. IQGAP2 binding is calcium dependent. GFP-IQGAP2 was immunoprecipitated from COS cells in the presence of cheleators (1 mM each), 1 mM $CaCl_2$, or from cells treated with 5 µM of the ionophore A23187 for 20 min. Co-purification of AKAP220 was assessed by RII overlay (top panel). (Mid and bottom panels) AKAP220 and GFP-IQGAP2 loading controls. (Below) Densitometry analysis of data in (A). Amalgamated data from three experiments, mean +/- SEM.

Fig. S3

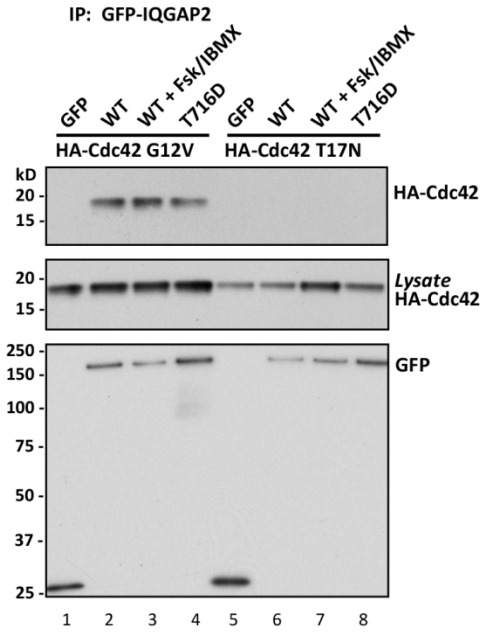

Fig. S3. Association of IQGAP2 with the Cdc42 GTPase is phosphorylation independent. Experiments were performed with (lanes 1 and 5) GFP alone, (lanes 2 and 6) wild-type IQGAP2 isolated from control cells, (lanes 3 and 7) wild-type IQGAP2 isolated from cAMP stimulated cells and (lanes 4 and 8) the IQGAP2 T716D mutant. **(**Top panels**)** Co-purification of HA-tagged G12V constitutively active Cdc42 mutant (lanes 1-4) or HA-tagged T17N dominant-interfering Cdc42 mutant (lanes 5-8). Loading controls for (middle) HA-Cdc42 mutants and (bottom) GFP-IQGAP2 are presented.

Fig. S4

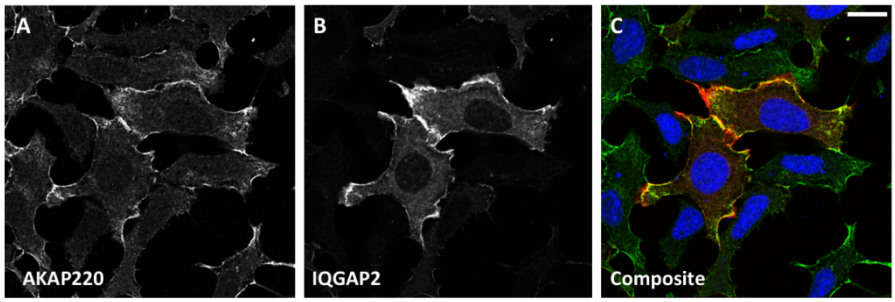

Fig. S4. AKAP220 and IQGAP2 co-distribute near the cell cortex. (A-C) Fluorescence detection of AKAP220 (**A,** green) and V5-IQGAP2 (**B,** red) in HEK-293 cells. Nuclei were stained with DRAQ5 as indicated in the composite image **(C)**. Scale bar indicates 20 µm.

Fig. S5

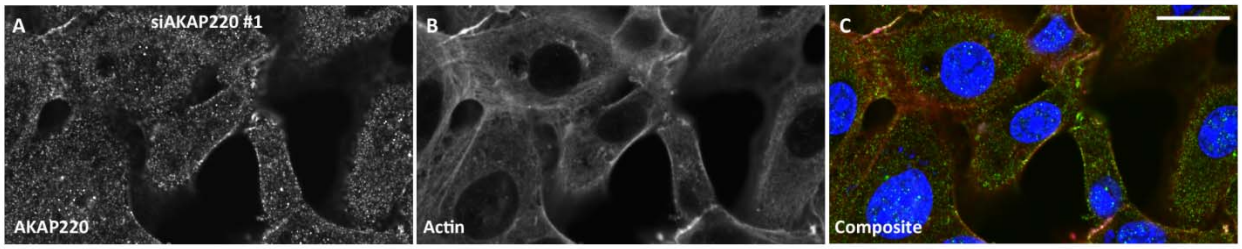

Fig. S5. AKAP220 knockdown affects levels of actin near the cell periphery. Staining patterns for AKAP220 **(A,** green**)** and actin **(B,** red**)** in cells treated with an independent siRNA towards AKAP220 **(A-C)**. Nuclei were stained with DRAQ5 as indicated in the composite image **(C)**. Scale bar indicates 20 µm.

Fig. S6

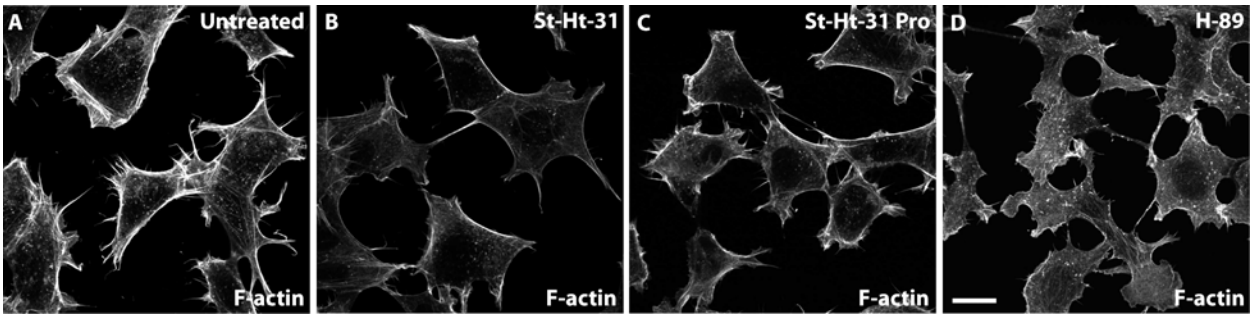

Fig. S6. Disruption of kinase anchoring and suppressing PKA activity impacts filamentous actin at the cell periphery. Fluorescently conjugated phalloidin was used to detect F-actin in untreated HEK-293 cells (A), treated with 10 μM stearated Ht-31 (St-Ht31) disruptor peptide (B), treated with 10 μM St-Ht31 proline mutant (St-Ht-31 Pro) control peptide (C) and cells treated with 10 μM of the PKA small molecule inhibitor H-89 (D). Cells were treated in each condition for 1 hour. Scale bar represents 20 μm.